Chapter 5: Wear

5.1 Introduction

This chapter aims to summarise literature on wear as it applies to the work of this thesis. It therefore concentrates on wear as experienced in cutting tests, i. e. the evaluation of the performance of samples when used as a tool tip in a lathe. Other forms of wear testing are largely excluded here.

The terminology used in cutting is illustrated in fig. 5-1.

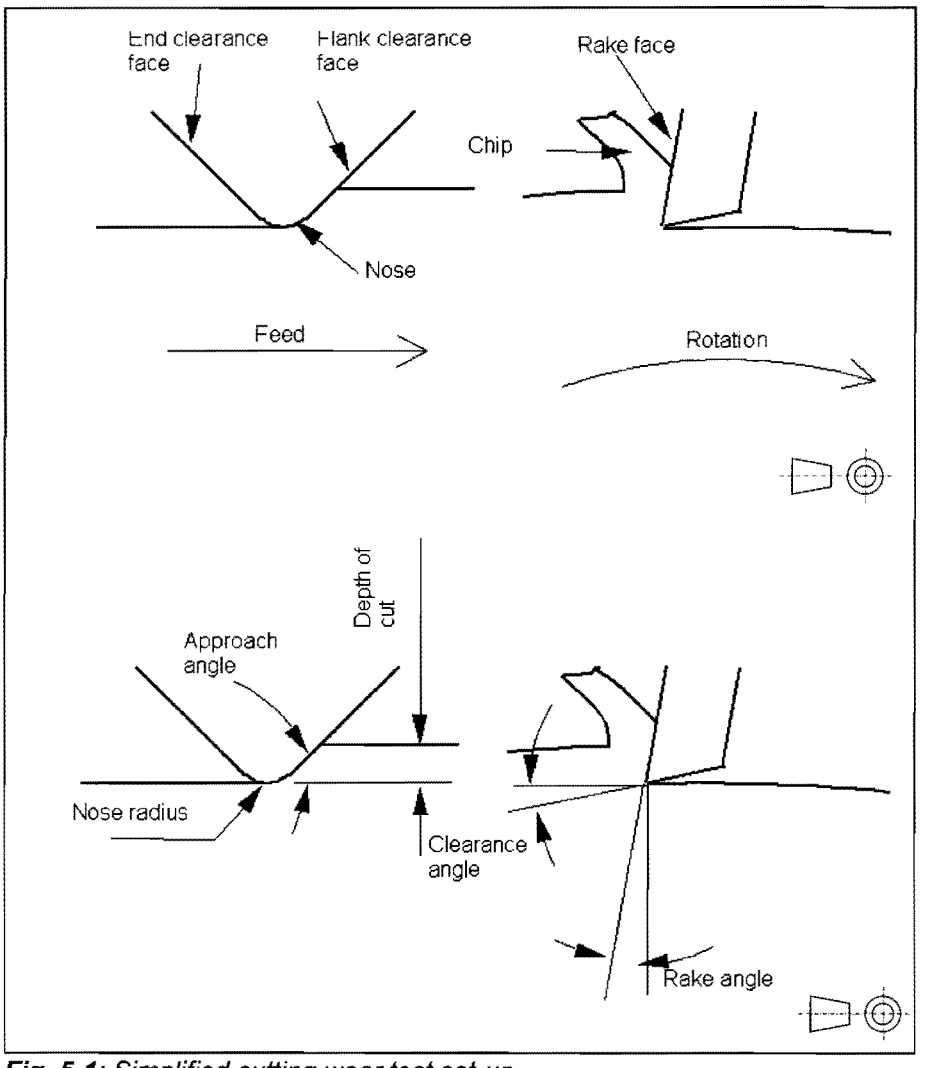

***Fig. 5-1**: Simplified cutting wear test set-up.*

5.2 Wear qualitatively

Wear is a complex phenomenon and several mechanisms contribute to the overall wear of a tool. During turning a cutting tool is subjected to friction, which results in high temperature, and various forces, causing high internal pressures and stresses in the tool. High temperature in turn results in chemical reactions at the interface between the insert and the workpiece. Three types of 'loading' are commonly identified: Mechanical, thermal and chemical (Stachowiak and Stachowiak, 1994).

Considerable confusion exists as to the terminology and classification of wear mechanisms in general (Blau, 1989; Hutchings, 1992; Lancaster, 1990). A satisfactory classification for ceramics is that of Stachowiak and Stachowiak (1994). Their classification, together with descriptions of the different wear mechanisms, is summarised in table 5-1.

***Table 5-1**: Wear mechanisms (Stachowiak and Stachowiak, 1994; Blau 1989).*

Mechanism		Description	Appearance of wear scar	Remarks
Mechanical wear	Abrasion	Wear caused by particles or protuberances forced against a surface	Grooves parallel to movement	Usually the dominating mechanism on the flank.
	Adhesive wear	Grains or groups of grains jerked from tool surface.	Rough.	Aggravated by weak interphase bonding in the tool
	Fracture	Ranges from complete catastrophic failure of the cutting edge to less severe chipping.		Caused by large thermal expansion and/or low thermal conductivity
Chemical wear		Chemical reaction between workpiece material and the tool leading to the formation of detrimental compounds in the tool.	Smooth.	

Wear damage on cutting tool inserts is divided into distinct wear features: Crater wear on the rake face, and flank and notch wear on the flank clearance face (fig. 5-2). Flank wear is caused by abrasive contact between the tool and the freshly cut workpiece. Notch wear is caused by fracture and occurs especially on brittle tools cutting hard materials. Crater wear is caused by contact between the chip and the rake face.

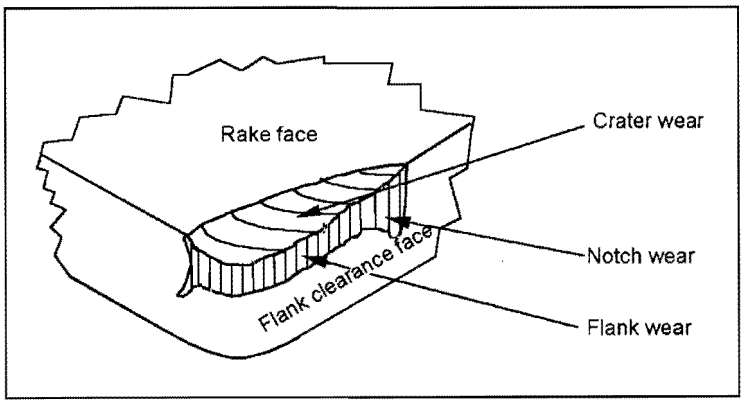

***Fig. 5-2**: Typical wear features on a cutting tool insert (see fig. 5-1 for feed direction and the position of the chip) (Stachowiak and Stachowiak, 1994).*

5.3 Testing

In industry the criterion for tool performance is its satisfactory performance. 'Satisfactory performance' can imply satisfactory surface finish and tolerance. In the extreme 'satisfactory performance' can even mean the lack of excessive vibration in the lathe or the non-occurrence of catastrophic failure of the tool (personal communications, Ravenhill and Jarvis). When testing an insert in the laboratory various measurements can be taken to evaluate an insert: Weight loss of the insert, surface roughness of the work piece and dimensions of the work piece and the insert can be measured (Li *et al*, 1993; Li *et al*, 1994; ISO 3685).

The performance of cutting tool inserts can be quantified in different ways. ISO 3685 recommends that the criterion for performance be the tool life. Tool-life is defined as the duration of time necessary for the span of some wear feature to reach a pre-decided value. Possible wear feature measurements are the depth of the flank wear V or the crater depth K as shown in fig. 5-3. For ceramics ISO 3685 recommends either a maximum flank wear width of 0.6 mm or an average flank wear of 0.3 mm as the pre-decided cut-off point for tool-life. With the ISO recommended work piece material (steel or cast iron), notch and crater wear should not occur on ceramic cutting tools (in the experimental work of this work, however, a ceramic rod of Siffer' is used as a workpiece material).

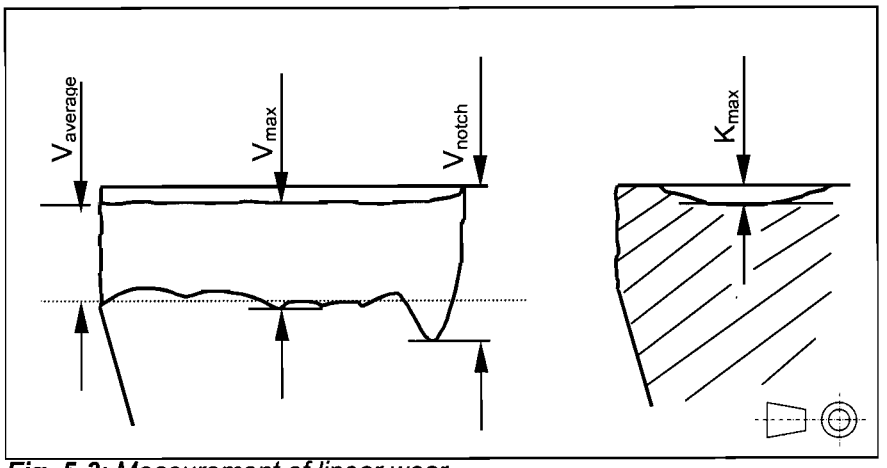

***Fig. 5-3**: Measurement of linear wear.*

5.4 Models

The Archard wear law is commonly used to describe to wear, particularly abrasive wear (Hutchings, 1992):

$$\frac{\delta Q}{\delta S} = \frac{k_A}{H} N \qquad (5\text{-}1)$$

where Q is the volume of material worn away after sliding a distance S. N is the normal force, H is the hardness (no particular hardness measurement value recommended) of the softer material and k_A is a coefficient that takes all other factors into account. The ratio $\delta Q/\delta S$ is commonly known as the specific wear rate.

Axén and Jacobson (1994) reformulated the Archard wear law to develop a model for the abrasive wear of composite materials. They defined wear resistance Ω as

$$\Omega = \frac{N}{\delta Q / \delta S} \qquad (5\text{-}2)$$

With this definition Archard's wear law can be reformulated as

$$\frac{\delta Q}{\delta S} = \frac{N}{\Omega} \qquad (5\text{-}3)$$

Axén and Jacobson propose two possible modes for composite wear. Firstly, equal wear mode in which two phases wear down at the same linear rate. Secondly, equal pressure wear mode in which both the hard and soft phase carry the same pressure. Equal wear and equal pressure mode should respectively give the lower and upper bounds of the wear rate, with the actual wear for a composite lying somewhere in between. For equal wear mode Axén and Jacobson derived the linear equation

$$\Omega_{Composite} = g_{Hard}\Omega_{Hard} + g_{Soft}\Omega_{Hard} \qquad (5\text{-}4)$$

and for equal pressure mode they derived the inversely additive equation.

$$\Omega_{Composite} = \frac{1}{\frac{g_{Hard}}{\Omega_{Hard}} + \frac{g_{Soft}}{\Omega_{Soft}}} \qquad (5\text{-}5)$$

where g_{hard} and g_{soft} is respectively the area fractions of the exposed hard and soft phases. For composites with randomly distributed phases the area fractions of phases are equal to the volume fractions, i.e. g = f. By combining equation 5-4 and 5-3 the wear under conditions of equal linear penetration can be derived as the inversely additive equation

$$\frac{\delta Q}{\delta S} = \frac{N}{f_{Hard}\Omega_{Hard} + f_{Soft}\Omega_{Hard}} \qquad (5\text{-}6)$$

where f is the volume fraction of the phases. By combining equations 5-5 and 5-3, the wear under equal pressure can be derived as the linearly additive equation

$$\frac{\delta Q}{\delta S} = N\left(\frac{f_{Hard}}{\Omega_{Hard}} + \frac{f_{Soft}}{\Omega_{Soft}}\right) \qquad (5\text{-}7)$$

Fig. 5-4 illustrates the trend of the bounds for the specific wear rate given by equations 5-6 and 5-7.

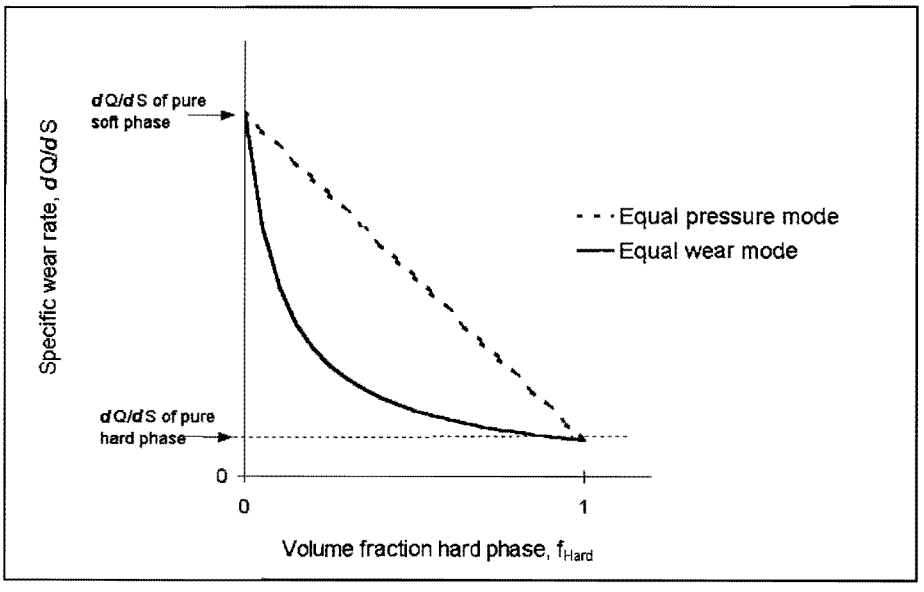

***Fig. 5-4**: Equal wear and equal pressure composite wear modes compared.*

The relations (equations 5-1 to 5-7) and of Archard and of Axén and Jacobson only describe the instantaneous wear rate and the coefficient k_A and wear resistance Ω are not constant, but change with time as wear progresses. In practice, wear typically follows the trend illustrated in fig. 5-5 (Jarvis, personal communication; Blau, 1989).

In the experimental work of this thesis no force measurements were taken. The relationship given by Singh and Vajpayee (1980) is therefore rather useful for interpretation of results. They state that the normal force on a cutting tool follows the simple relationship

$$N = k_{SV1}V + k_{SV2} \qquad (5\text{-}8)$$

where k_{SV1} and k_{SV2} are constants. At the least this relationship shows that the normal force on the tool shows a linear increase, and not, for instance, a sudden exponential jump at any stage.

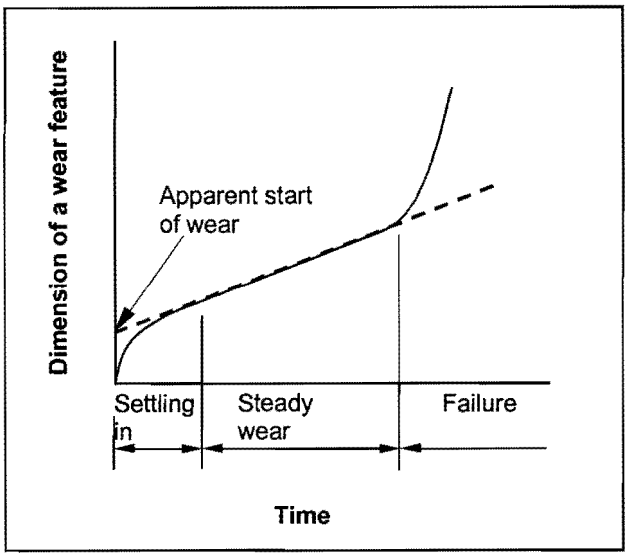

***Fig. 5-5**: Typical course of wear.*

5.5 The influence of hardness and toughness on wear

Hardness and toughness are the two most important factors in wear resistance (Hickman, personal communication). This relationship can be quantified by Baldoni *et al*'s (1986) wear resistance indicator $K_{IC}^{3/4}H^{1/2}$ (K_{IC} being mode I fracture toughness and H hardness) which indicates abrasive wear resistance. Mode I fracture toughness, K_{IC} ('K one C', i.e. mode I fracture toughness) and not K_c ('K C'), is specified but it is unclear if Baldoni *et al* actually used K_{IC} values. Baldoni *et al* seem to have used Knoop hardness. It is unclear how accurate the wear resistance indicator will be with other forms of toughness and hardness measurements, like it used in this work. In this work it is used with Vickers' hardness, H_V and Vickers' crack length toughness K_C, i.e. as $K_C^{3/4}H_V^{1/2}$.

Toughness can be determined from indentation crack length, for which several equations exist (McColm, 1990). In their work on diamond-alumina Noma and Sawaoka (1984 and 1985) used the relation of Lawn *et al* (1980):

$$K_C = 0.0070\, E^{1/2} H_V^{1/2} d^2 c^{-3/2} \qquad (5\text{-}9)$$

with the dimensions c and d as defined in fig. 5-6. (If c and d are in m and E and H_V is in Pa then K_c is in $Pa.m^{½}$.) As Noma and Sawaoka used this equation for a similar material, it seems reasonable to use it in

this work as well. The Young modulus (E) for the composites in this work is estimated as 490 GPa (appendix A4).

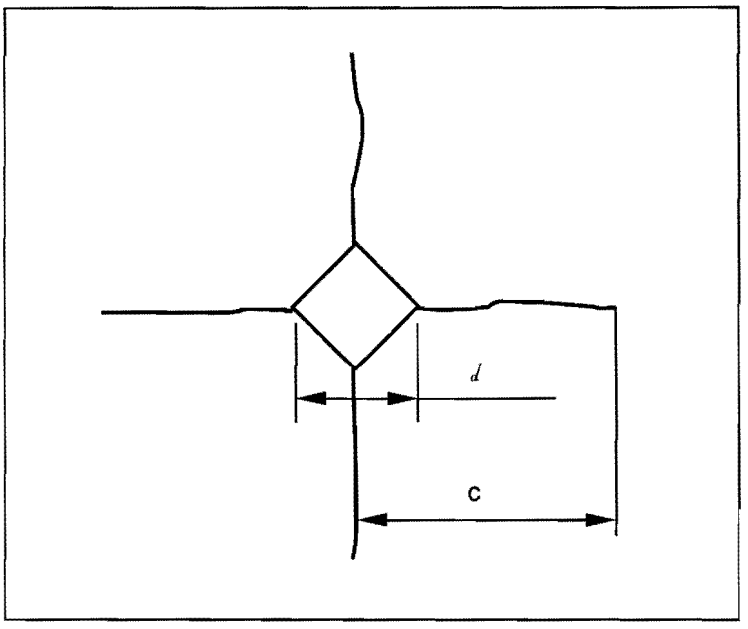

***Fig. 5-6**: Indentation dimensions used in toughness measurement.*

5.6. Wear and wear related properties of relevant materials

5.6.1 Untoughened alumina

Alumina exhibits increased hardness with smaller grain size as illustrated in fig.5-7.

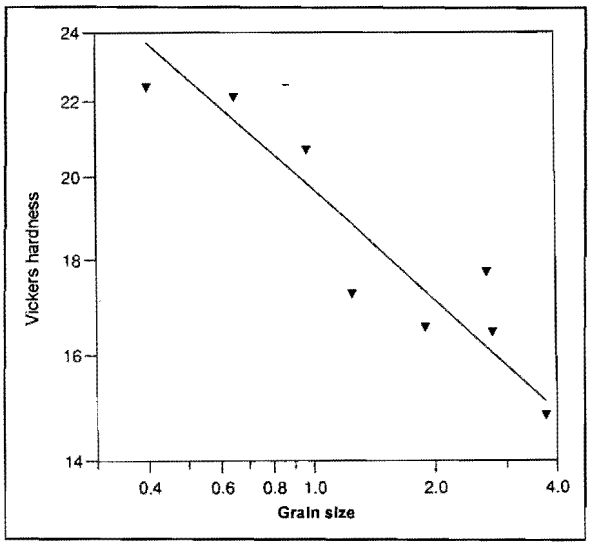

***Fig. 5-7**: Grain size dependence of the Vickers hardness (at 10 kg f) of alumina (Krell and Blank, 1995).*

Pure alumina or alumina only containing sintering aids is not very resistant to thermal loading (differential heating) due to its relatively low thermal conductivity, which drops of between 25 °C and 400 °C (fig. 5-8). Alumina for cutting use is normally toughened with some additive, like zirconia, although untoughened alumina is sometimes used in industry (Toshiba marketing pamphlet, Dörre and Hübner, 1984).

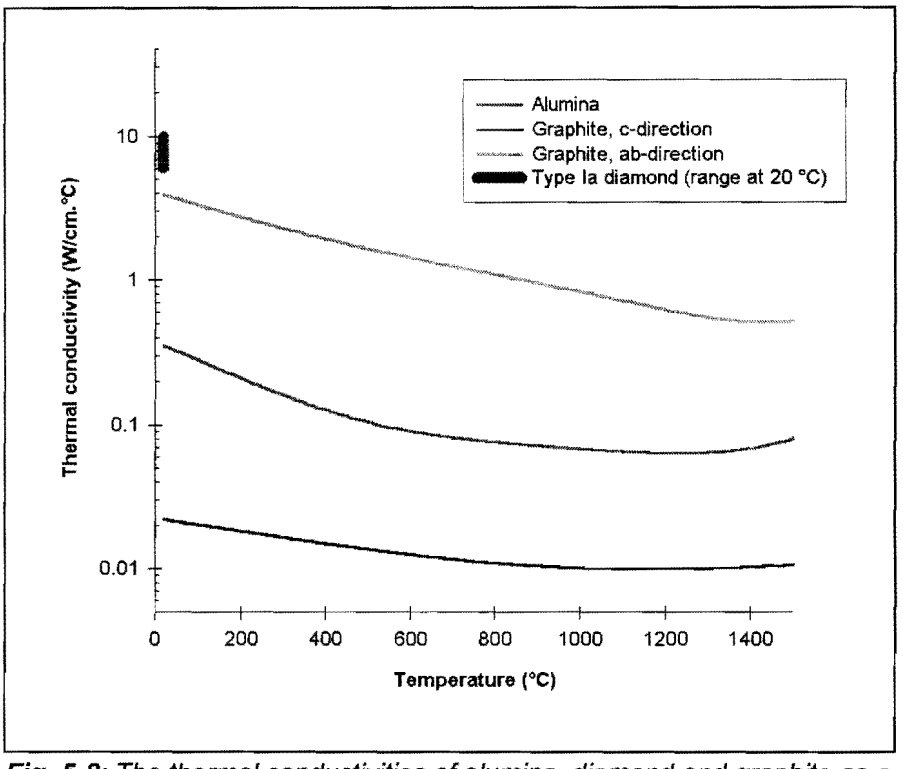

***Fig. 5-8**: The thermal conductivities of alumina, diamond and graphite as a function of temperature. Data from Dörre and Hübner (1984) and Pierson (1993). No data for any form of diamond at higher temperature than shown are available.*

Alumina in general displays good resistance to chemical loading by ferrous alloys. Some reactions occur when cutting oxides of calcium, magnesium and silicon and with titanium alloys (Stachowiak and Stachowiak, 1994).

Typical wear features of non-toughened alumina are shown in fig. 5-9. Alumina shows relatively little cratering in turning, but it shows broad flank wear. Like some other ceramics alumina has its most optimal wear at high speed, typically above 100 m/min, as fig. 5-10 shows (Dörre and Hübner, 1984).

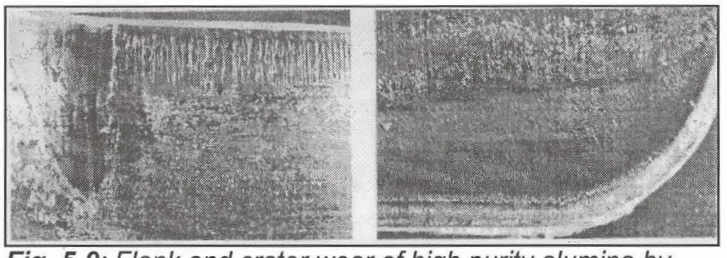

***Fig. 5-9**: Flank and crater wear of high purity alumina by abrasion, presumably after cutting metal. ×8.5. (Dörre and Hübner, 1984).*

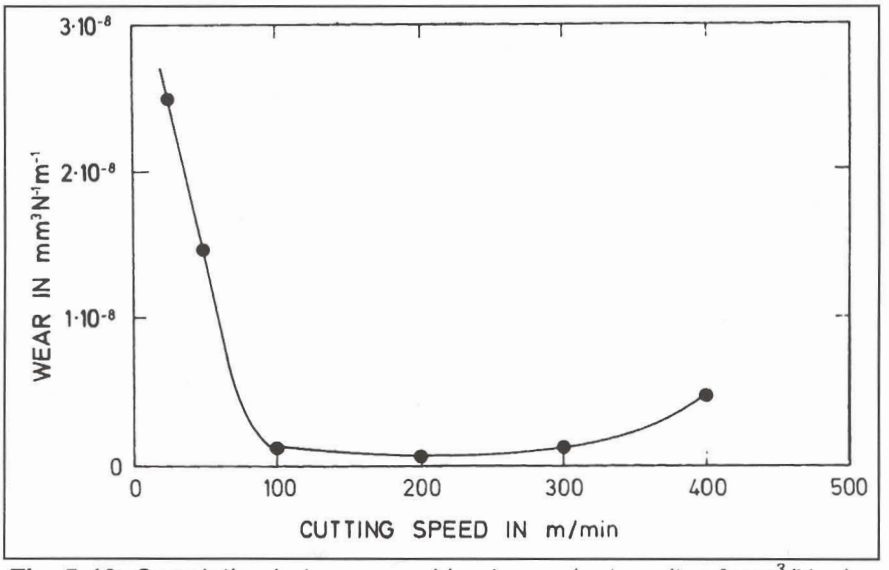

***Fig. 5-10:** Correlation between combined wear (note units of $mm^3/N.m$) and cutting speed of high purity alumina (Dörre and Hübner, 1984), presumably on cast iron or steel.*

5.6.2 Diamond-alumina composites

Reinforcement of matrices for cutting purposes with the inclusion of inert, non-whisker, non-platelet particles is not common. (In this sense 'inert' means materials that do not change in composition or phase during processing like zirconia does). For instance, Chuanzhen and Xing (1996) developed alumina (matrix) composites with silicon carbide enforcement in the form of both simply shaped, relatively spherical particles and whiskers. However they only subjected their whisker containing composites to cutting tests, presumably because of its toughness being double that of the composites with simple particles (8.1 $MPa.m^{½}$ versus 4.9 $MPa.m^{½}$).

In sharp contrast with alumina, diamond has excellent thermal conductivity (fig. 5-8), the highest of any solid at room temperature. For a finely dispersed, isotropic composite, with no thermal barrier between phases, thermal conductivity k is linearly additive with respect to volume fraction f, i.e.

$$k_{Composite} = f_{Diamond} k_{Diamond} + f_{Alumina} k_{Alumina} \qquad (5\text{-}10)$$

Addition of diamond therefore has the potential of enhancing an alumina matrix's thermal conductivity. This would result in less sharp temperature gradients and improve the ability to resist thermal loading. However, there can be some doubt about to what extent the ideal situation of equation 5-10 would be followed in reality. Even in the case of perfect mechanical contact between phases a thermal barrier can exist between phases. Hasselman *et al*'s work (1994) on a diamond-cordierite composite indeed showed that the above ideal additive effect for composites was not followed in their composites: Composite thermal conductivity was approximately a factor of ten smaller than that predicted by equation 5-10. In the case of the diamond-alumina of this work the possible formation of a graphite layer between diamond and alumina therefore provides two possible mechanisms for resistance to conduction of heat:

1) Two phase boundaries (diamond to graphite and graphite to alumina, instead of only diamond to alumina) which leads to two possible phase to phase thermal barriers.

2) Depending on the predominant orientation in the graphite layer, the graphite layer itself can have low thermal conductivity. In the worst possible scenario the graphite layer can form on the diamond with its ab-direction parallel to the diamond surface. This would imply heat transfer in the c-direction, in which thermal conductivity is very low (fig. 5-8). (It is more likely, however, that the graphite would be isotropic and that its thermal conductivity would be intermediate to that of the c and ab-directions. Thermal conductivity in the ab-direction is good, better than alumina, as can be seen in fig. 5-8).

Noma and Sawaoka (1985a and 1985b) manufactured diamond alumina composites and determined their hardness and toughness. Interestingly, they intentionally and extensively graphitised the diamond in their composites to take advantage of a toughening effect of the conversion of diamond to graphite. Grain size in their alumina matrix was relatively coarse, being > 2 μm. In Noma and Sawaoka's results it seems that hardness was sacrificed with increasing diamond content but that hardness was roughly independent of graphitisation (fig. 5-11). Toughness achieved as functions of diamond content and increased graphitisation (longer heat treatment leading to more graphitisation, also compare fig. 4-5) is seen in fig. 5-12 and 5-13. The obvious toughening mechanism would be microcrack toughening due to volume expansion (the specific volume of carbon particles changes from the 0.32 cm^3/g of diamond to the 0.44 cm^3/g of graphite). However, Noma and Sawaoka also observed an increase in the aspect ratio (ratio of the length to width) of carbon particles, and they suggest crack deflection by this change as the toughening mechanism. (Noma and Sawaoka's experimental conditions are summarised in table 4-3.)

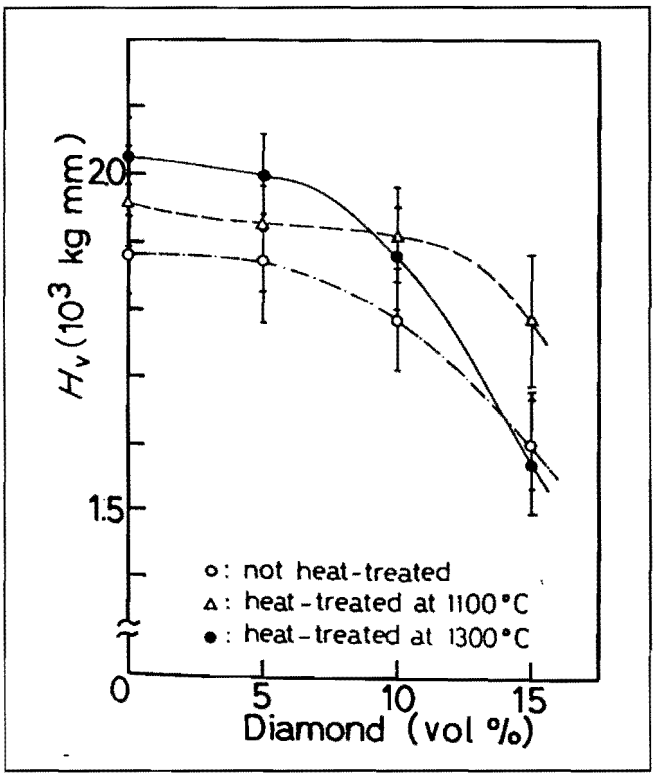

***Fig. 5-11**: Hardness as a function of diamond content after post densification heat treatment of 6h. Indentor load 10 kg. From Noma and Sawaoka (1984)*

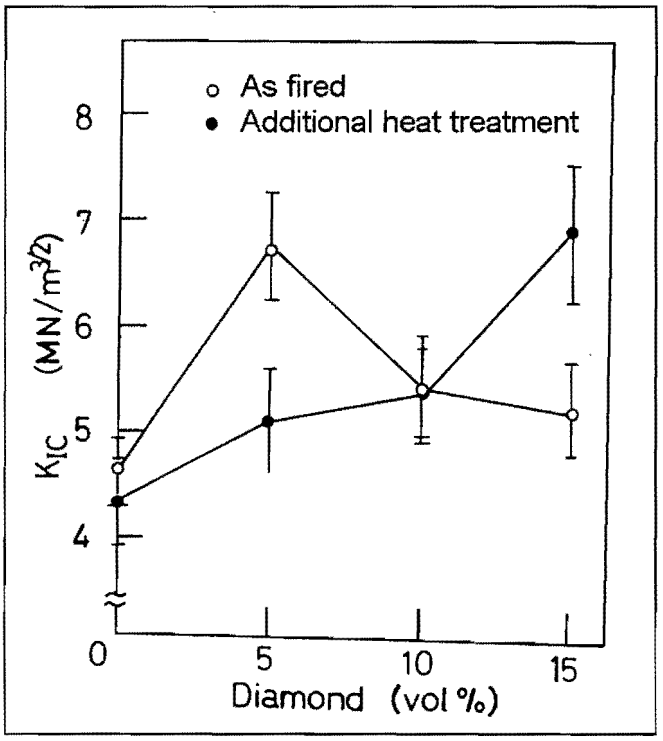

***Fig. 5-12**: Variation of fracture toughness with diamond content. Method of toughness measurement not given. Heat treatment was 6 h at 1 300 °C. From Noma and Sawaoka (1985).*

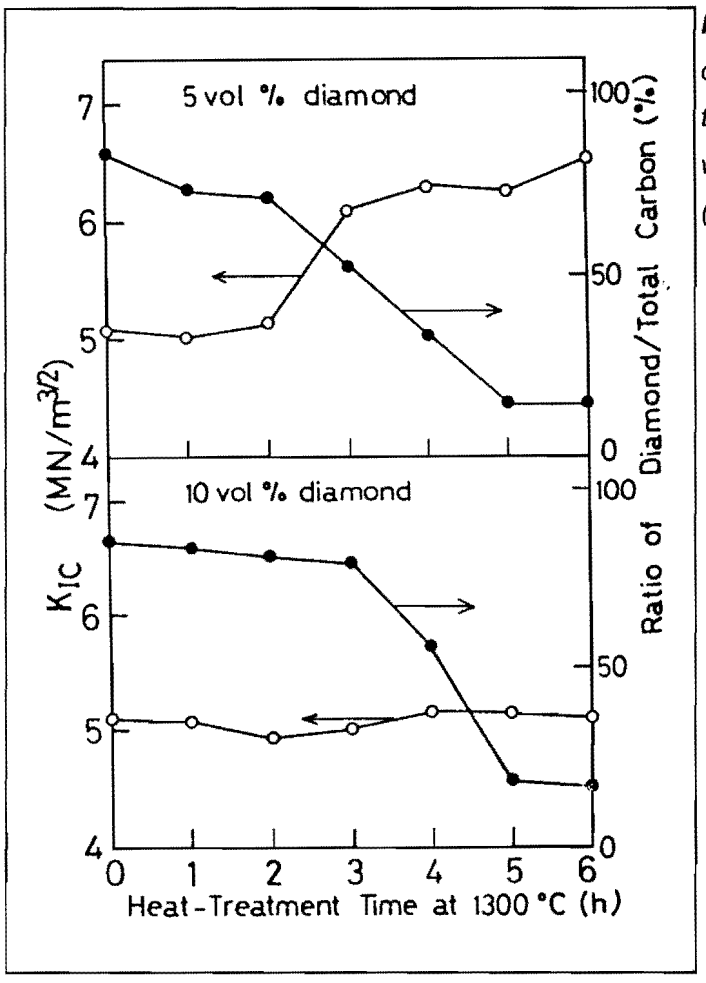

***Fig. 5.13**: Variation of fracture toughness and degree of graphitisation with post-firing heat treatment. Fracture toughness by indentation with a 30 kg load. From Noma and Sawaoka (1985).*

The only available literature on the wear of actual diamond-alumina composites is that of Chu *et al* (1992). They manufactured a diamond-alumina composite by dry pressing followed by hot pressing at 1 550 °C. The resultant composite's friction coefficient was compared with that of diamond and zirconia toughened alumina. An increase in the coefficient of friction implied an increase in wear. However, their test on a magnetic disk is extremely mild compared to the wear test method employed in this work. In the face of the lack of other wear data on diamond-alumina composites their data are included and given in fig. 5-14. Diamond-alumina is seen to have an advantage in having friction coefficients of approximately less than halve of that of zirconia-alumina.

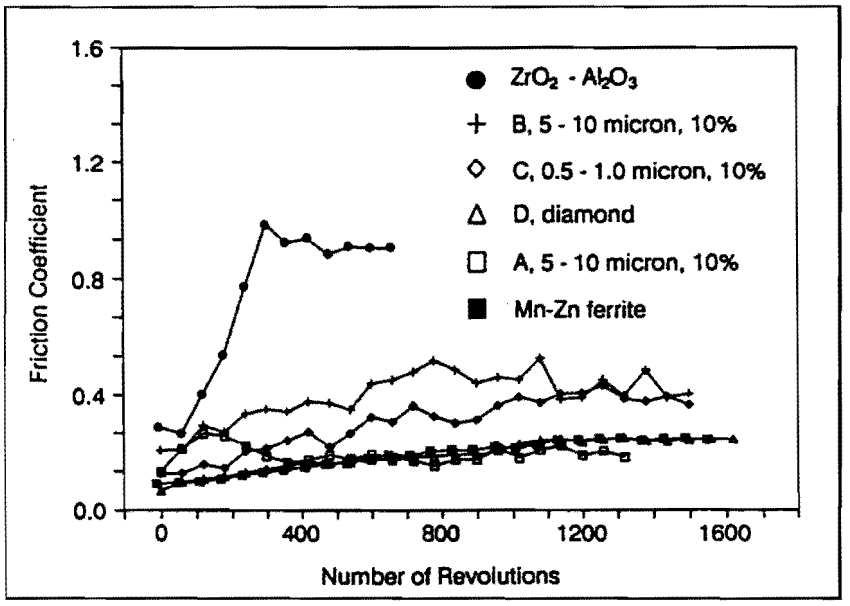

***Fig. 5-14**: The friction coefficient of a diamond-alumina composite on a magnetic storage disk compared to some other materials. Indicated sizes and percentages in the legend refer to the size and volume percentage of diamond (Chu* et al, *1992).*